Correlation between relaxations and plastic deformation, and elastic model of flow in metallic glasses and glass-forming liquids

Wei Hua Wang (汪卫华)[1]
Institute of Physics, Chinese Academy of Sciences, Beijing 100190, People's Republic of China

(Received 2 March 2011; accepted 1 August 2011; published online 14 September 2011)

We study the similarity and correlations between relaxations and plastic deformation in metallic glasses (MGs) and MG-forming liquids. It is shown that the microscope plastic events, the initiation and formation of shear bands, and the mechanical yield in MGs where the atomic sites are topologically unstable induced by applied stress, can be treated as the glass to supercooled liquid state transition induced by external shear stress. On the other hand, the glass transition, the primary and secondary relaxations, plastic deformation and yield can be attributed to the free volume increase induced flow, and the flow can be modeled as the activated hopping between the inherent states in the potential energy landscape. We then propose an extended elastic model to describe the flow based on the energy landscape theory. That is, the flow activation energy density is linear proportional to the instantaneous elastic moduli, and the activation energy density ρ_E is determined to be a simple expression of $\rho_E = \frac{10}{11}G + \frac{1}{11}K$. The model indicates that both shear and bulk moduli are critical parameters accounting for both the homogeneous and inhomogeneous flows in MGs and MG-forming liquids. The elastic model is experimentally certified. We show that the elastic perspectives offers a simple scenario for the flow in MGs and MG-forming liquids and are suggestive for understanding the glass transition, plastic deformation, and nature and characteristics of MGs © *2011 American Institute of Physics*. [doi:10.1063/1.3632972]

I. INTRODUCTION

The slow down of flow or glass transition phenomena, which is a universal property of supercooled liquids when they are cooled rapidly enough, have attract extensive studies due to their scientific significance for understanding the nature of the condensed matter and wide applications.[1–8] For crystalline alloys, their properties and characteristics can be understood in microstructure including the crystal structure, the degree of order, and the contents and distributions of defects such as dislocations and grain boundaries. While the "many-body" random structural nature of glasses is quite difficult to be described or detected accurately like their crystalline counterpart.[1–9] It is therefore a major challenge to understand their formation and deformation and to establish their structure-properties relationship. The recently developed bulk metallic glasses provide model glassy systems for investigating the glass transition, properties, and plastic deformation of glasses.[10–20]

The systematical elastic property studies indicate that the elastic moduli can be used as leading parameters for understanding and describing the most fundamental issues in MGs.[15,17–20] The properties, formation, features, and plastic flow of MGs show clear correlation with their elastic constants.[17] It is recently certified that the glass transition, relaxation, and homogeneous, and inhomogeneous deformation in glasses might be all closely related to flow event controlled by activation energy.[7,13,16] It therefore desires to describe and model the flows in MGs in elastic perspectives, which will be helpful for establishing a united and simple physics picture for the plastic deformation and glass transition based on few readily measurable physical parameters such as elastic moduli.

In this paper, the compelling experimental evidences are shown to demonstrate that the plastic flow and the relaxations in MGs are directly related through elastic moduli. The plastic events, shear banding, and mechanical yield are actually the localized glass to supercooled liquid transition driven by shear stress. Based on the experimental observations, the glass formation from solidification of liquid, the mechanical deformation, relaxations, and stability of glasses are treated as the flow phenomenon, and the flow is modeled as the change of the configurations or activated hopping between inherent states in the potential energy landscape. An extended elastic model is proposed to describe both homogeneous flow in MG-forming liquids and inhomogeneous flow in MGs. The elastic perspectives, which consider all MGs and MG-forming liquids exhibit universal behavior based on the readily measurable parameters of elastic moduli, are provided to understand the glass transition and plastic deformation in the MGs and MG-forming liquids.

II. EXPERIMENTAL

The bulk MGs samples were prepared by a copper mold suction casting method and the amorphous ribbons were obtained by melt spinning technique.[20,21] The glassy nature was identified by X-ray diffraction (XRD), and differential scanning calorimetry (DSC) performed under a purified argon atmosphere in a Perkin-Elmer DSC-7. The MGs chosen (listed in Tables I and II) had a wide range of glass transition temperature, T_g and significantly different in physical and

[1]Electronic mail: whw@iphy.ac.cn.

 © 2011 American Institute of Physics

Author complimentary copy. Redistribution subject to AIP license or copyright, see http://jap.aip.org/jap/copyright.jsp

mechanical properties.[16,19,21]The specific heat measurement was performed in Perkin-Elmer DSC7 calibrated for temperature and enthalpy at various heating rates with high-purity indium and zinc under protection of a purified argon atmosphere.

Dynamic mechanical spectroscopy (DMS) measurements were performed using TA Inc. dynamic mechanical analyzer (DMA) Q800 by single-cantilever bending method for rod samples and film tensile method for ribbons in a nitrogen-flushed atmosphere. The storage modulus E' and loss modulus E'' were measured by temperature ramp mode at a heating rate of 2 K/min. Uniaxial compression tests at room temperature (RT) were performed on an Instron 5500R1186 machine. Tests were carried out in a constant-crosshead-displacement-rate controlled manner. The samples with gauge aspect ratio (height/diameter) of 2:1 were cut out of the as-cast rods, and the two ends were polished to make them parallel to each other prior to the compression test. For each sample, sets of five measurements are repeated in compression tests.

Elastic moduli of the MGs were monitored using ultrasonic method. The amorphous rod ($\varphi = 3$–8 mm) was cut to a length of about 8 mm, and its ends were carefully polished flat and parallel. The acoustic velocities (longitudinal and transverse velocities v_l, v_s) were measured using a pulse echo overlap method by a MATEC 6600 model ultrasonic system with a measuring sensitivity of 0.5 ns.[16] The excitation and detection of the ultrasonic pulses were provided by X- or Y-cut (for longitudinal and transverse waves, respectively) quartz transducers. The frequency of the ultrasonic is 10 MHz. The density was determined by the Archimedean technique and the accuracy lies within 0.1%. The velocities measurements were repeated for the each sample for several times to examine the reproducibility and minimize error. Elastic constants (the Yong's modulus E, the shear modulus G, and the bulk modulus K and Poisson's ratio v) were derived from the density and acoustic velocities as follow: $G = \rho v_s^2$; $K = \rho\ (v_l^2 - 4/3\ v_s^2)$; $v = \rho(v_l^2 - 2v_s^2)/2(v_l^2 - v_s^2)$; $E = 2\ G(1 + v)$.

III. RESULTS AND DISCUSSION

We start from the investigation of the relationships among the microscope plastic events, plastic deformation, yield, relaxations, and glass transition. Microscopically, the plastic deformation of MGs is regarded as a consequence of formations and self-organizations of shear plastic flow events. The shear transformation zone (STZ) theory[11] was proposed to model the plastic events of MGs, which suggests

TABLE I. Data of average atomic volume v*, Poisson's ratio ν, shear modulus G, Debye frequency f, and yield stress σ_y, and the critical stress σ_c of various MGs (Refs. 13, 14, 16, 20 and 34).

Alloy composition	v* (10^{-29}m^3)	v	G (GPa)	f (10^{12}Hz)	σ_y (GPa)	σ_c (GPa)
1. Ca65Zn16.5Mg8.5Li10	3.362	0.306	8.9	4.595	0.53	0.33
2. Ce70Al10Ni10Cu10	2.813	0.313	11.5	2.997	0.65	0.41
3. La55Al25Cu10Ni5Co5	2.639	0.342	15.6	3.773	0.85	0.50
4. Mg65Cu25Gd10	1.949	0.320	18.6	5.539	0.98	0.63
5. La55Al25Co20	2.718	0.327	15.4	3.769	0.99	0.48
6. Au55Cu25Si20	1.767	0.417	24.6	3.837	1.00	0.83
7. Pr55Al25Co20	2.502	0.324	17.4	3.927	1.01	0.53
8. Au49.5Ag5.5Pd2.3Cu26.9Si16.3	1.748	0.406	26.5	4.093	1.20	0.86
9. Pt60Ni15P25	1.413	0.420	33.8	4.274	1.40	1.09
10. Cu46Zr54	1.711	0.391	30.0	5.401	1.40	0.90
11. Pt57.5Cu14.7Ni5P22.8	1.437	0.434	33.4	4.302	1.45	1.09
12. Pd77.5Cu6Si16.5	1.452	0.409	31.8	5.040	1.50	1.03
13. Pd64Ni16P20	1.376	0.405	32.7	5.277	1.55	1.07
14. Zr57.5Nb5Cu15.5Ni12Al10	1.959	0.379	30.8	5.654	1.58	0.84
15. Cu46Zr42Al7Y5	1.698	0.364	31.0	5.630	1.60	0.89
16. Zr55Ti5Cu20Ni10Al10	1.852	0.375	31.0	5.724	1.63	0.86
17. Zr64.13Cu15.75Ni10.12Al10	1.939	0.377	28.5	5.415	1.69	0.81
18. Pd60Cu20P20	1.405	0.409	32.3	5.295	1.70	1.06
19. Pd40Cu30Ni10P20	1.319	0.399	34.5	5.725	1.72	1.12
20. Pd40Cu40P20	1.325	0.402	33.2	5.609	1.75	1.10
21. Zr46.75Ti8.25Cu7.5Ni10Be27.5	1.648	0.359	35.2	6.845	1.83	0.96
22. Zr41.2Ti13.8Ni10Cu12.5Be22.5	1.690	0.352	34.1	6.542	1.86	0.92
23. Cu57.5Hf27.5Ti15	1.555	0.356	37.3	5.428	1.94	1.01
24. Zr48Nb8Ni12Cu14Be8	1.705	0.367	34.3	6.146	1.95	0.93
25. Cu64Zr36	1.513	0.352	34.0	5.791	2.00	0.98
26. Zr55Al19Co19Cu7	1.900	0.352	37.6	6.438	2.20	0.90
27. Cu50Hf43Al7	1.667	0.358	42.0	5.341	2.20	1.03
28. Ni45Ti20Zr25Al10	1.596	0.359	40.2	6.952	2.37	1.03
29. Ni40Ti17Zr28Al10Cu5	1.615	0.349	47.3	7.453	2.59	1.09
30. Ni60Nb27.2Ta6.8 Sn6	1.436	0.357	59.4	7.283	3.50	1.30
31. Ni60Nb35Sn5	1.416	0.385	66.3	8.024	3.85	1.41
32. Fe53Cr15Mo14Er1C15B6	1.292	0.320	75.0	9.742	4.20	1.47

Author complimentary copy. Redistribution subject to AIP license or copyright, see http://jap.aip.org/jap/copyright.jsp

that a flow event is initiated from rearrangements of atoms in local regions, which contain tens of atoms.[11,12] The self-organization of the STZs forms the shear bands, and the propagation of the shear bands induces the yield, cracks, and the failure of the MGs.[10]

The underlying relaxations of glassy materials and supercooled liquids are governed by two main processes, the primary relaxation (α-relaxation) and the secondary relaxation (slow β-relaxation).[4] The α-relaxation involves large scale rearrangements of materials, and the activation of which makes the liquid flow. The α-relaxation is the principal source of information about the dynamics of glassy state, and the underlying flow during glass transition is mainly governed by the kinetic process of the α-relaxation. The slow β-relaxation,[22] which has been proved to be an intrinsic and universal feature of MGs, is regarded as a unit event of α-relaxation and is usually related to localized translational motions with cooperative nature, a reminiscent of plastic events in MGs. Experimentally, the activation energy of the β-relaxations of MGs, E_β, can be determined either by DSC or by DMS.[23,24]

Theories and models relate yielding and plastic deformation of glassy materials to their relaxations.[13,25,26] It is considered that the cooperative motions of atoms that are responsible for β-relaxation accommodate the deformation. In some polymer glasses, the transition of deformation modes (e.g., from brittle to ductile) often correlated with the β-relaxations.[27] The activation of isolated STZ is assumed to be associated with the β-relaxation,[13,28] while more experimental evidences are need to confirm the ideas in MGs.

A. Relations among the yield, plastic deformation, relaxation, and glass transition in MGs

1. The characterization of yielding in MGs

For crystalline materials, the onset of yielding marks the motion of dislocations at the atomic scale.[29] When a shear stress τ is applied to a material, two internal stresses will respond: long-range internal stress τ_G, which is mainly determined by the shear modulus G, and short-range internal stress τ_p, which mainly comes from the Peierls stress.[29] In the case of MGs, since there is no long-range ordered microstructure, the long-range internal stress is absent and only the short-range stress operates. A malleable MG, when compressed or rolled, can flow plastically under macroscopic yield stress σ_y due to the absence of strain hardening.[29] There have been sporadic reports that the onset of yielding in MGs actually takes place below the experimentally macroscopic yield strength,[30] and the plastic deformation could proceed at $0.9\sigma_y$ at RT without apparent formation of shear bands.[30,31] However, the nature of yielding in MGs received little attention and remains unclear yet. We reexamine the concept of elastic strain and the onset of yielding of the MGs based on the free volume model.[12] The aim is to understand the yield and its relation with the transition between the glass and its supercooled liquid. A critical value of free volume is found to be a sufficient condition for the yielding, which is similar to the critical value change of free volume during glass transition in MGs.[32–34]

The reduced free volume (RFV) is defined as, $x = V_f/\alpha V*$, where V_f is the average free volume per atom, α is a geometric factor between 0.5 and 1, $V*$ is the critical volume of an atom. Then, the net rate of increase of the average free volume per atom, v_f, is the difference between the increase rate of V_f caused by shear-induced dilatation and the decreasing rate of V_f caused by diffusion-induced annihilation:[12]

$$\dot{x} = \frac{f}{\alpha V^*}\exp\left(-\frac{\Delta G^m}{k_B T}\right)\exp\left(-\frac{1}{x}\right)\left\{\frac{2k_B T}{S}\frac{1}{x}\left[\cosh\left(\frac{\tau \bar{V}}{2k_B T}\right)-1\right]-\frac{V^*}{n_D}\right\}, \quad (1)$$

where f is the frequency of atomic vibration; k_B, the Boltzmann constant; T, the temperature, $\bar{V}$, the atomic volume ($\sim 1.25V*$); ΔG^m is the activation energy of atomic motion; and $S = \frac{2}{3}G\frac{1+\nu}{1-\nu}$, where v is Poisson's ratio, n_D is the number of diffusive jumps to annihilate a free volume equal to $V*$, which is between 1 and 10.

For most bulk MGs, they have a density difference of ~1% compared to that of their crystalline counterpart.[5,12,16] If the increment of density is entirely ascribed to the annihilation of free volume, the x_0 for most MGs would be in the order of ~1%. (The α is then taken to be 1.) While the initial value of RFV x_0 is adopted to be 2.2% here for two reasons:[32] (1) A smaller x_0, for example, 1.0% or 1.5% needs a geological time scale for the evolution of FRV to produce a change, which is inconsistent with experimental observations; (2) the probability $p(x)dx$ of finding an atom with RFV between x and $x+dx$ is$p(x)dx = c_1\exp(-c_2 x)dx$ (Ref. 12), where $c_1$and c_2 are constant. We have checked the critical value x_c depending on the change of the initial value of RFV x_0 *in Zr- and Cu-based MGs, and find that* x_c is independent of the change of x_0.

The numerical calculated results of Eq. (1) using the parameters listed in Table I for typical $Fe_{53}Cr_{15}Mo_{14}Er_1C_{15}B_6$ (Fe-MG), $Zr_{55}Ti_5Cu_{20}Ni_{10}Al_{10}$ (Zr-MG), and $Pt_{57.5}Cu_{14.7}Ni_5P_{22.8}$ (Pt-MG) with $\Delta G^m = hf$ (h is Planck constant), $\alpha = 1$ and $n_D = 3$ are shown in Fig. 1. It can be seen that the RFV sharply increases (becomes diverge) when it reaches a critical value of ~2.4%. The numerical result is independent of the chemical composition and mechanical parameters as well as the ΔG, n_D, α, and x_0 of different MGs. In other words, a critical value of $x_C \sim 2.4\%$ for the onset of yielding appears to fit for various MGs. The increase in free volume over x_C will drastically reduce the viscosity the alloy[12] and causes the flow of the MG. This result has also been confirmed by molecular dynamics simulation and elastostatic compression.[31]

Since a MG is expected to yield as the RFV reaches the critical value x_C, this indicates that the effective stress may not necessarily correspond to the experimentally measured macroscopic yield strength. To confirm the prediction, the evolution of x during deformation in Eq. (1) is checked. During deformation, the free volume gradually increases (i.e., $\dot{x} > 0$) until it reaches x_C, at which $\dot{x} = 0$ and the shear stress τ reaches a critical value τ_C determined from Eq. (1) as[12]

Author complimentary copy. Redistribution subject to AIP license or copyright, see http://jap.aip.org/jap/copyright.jsp

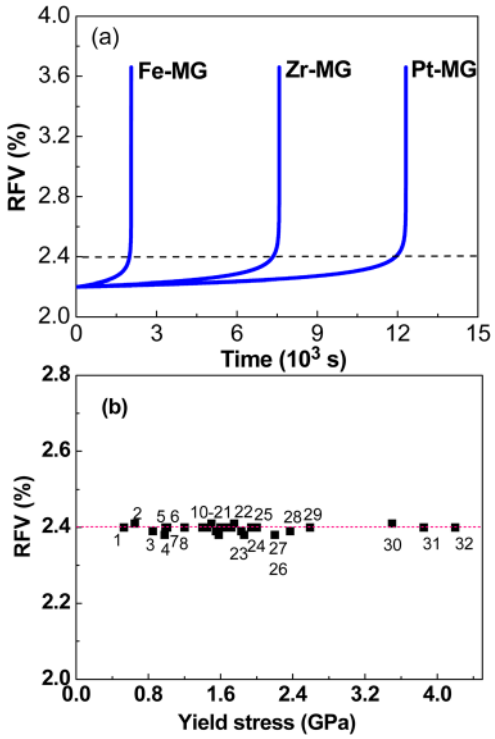

FIG. 1. (Color online) (a) The evolution of RFV in three typical Fe-, Zr-, Pt-MGs under shear with time with the parameters $\alpha = 1$ and $n_D = 3$. (b) The calculated critical values of reduced free volume x_c for 32 MGs listed in Table I.

$$\tau_c = \frac{2kT}{\Omega}\cosh^{-1}\left(\frac{x_C S}{2kT}\frac{V^*}{n_D} + 1\right). \quad (2)$$

Substituting $x_C \sim 2.4\%$ into Eq. (2), the τ_c can be obtained ($n_D$and T taken to be 3 and 300 K, respectively). The calculated σ_c ($\sigma_c \sim 2\tau_c$) and σ_y of a number of MGs are listed in Table I. It is apparent that $\sigma_c < \sigma_y$, the prediction is consistent with the experimental observations that the very stress for the onset of yielding is usually smaller than the macroscopic yield strength.[30,31,35] This demonstrates that when an applied stress satisfying Eq. (2), x will grow to ~2.4%, and the MG will yield provided it is loaded for sufficiently a long time. Even in crystalline alloys, the value of x cannot exceed a maximum value of x_m either, because the alloy would transit into liquid state or suffer a failure when $x > x_m$. Therefore, if $x > x_C$, the MGs would be in the supercooled liquid state.[12,36]

The existence of critical RFV value x_c at yield of MGs can be understood in the viscosity point of view. The relation between free volume and viscosity of MG-forming liquids is expressed as:[12] $\eta \propto \exp(1/x)$. Thus, the existence of a universal $x_C \sim 2.4\%$ for the onset of yielding indicates that there is a critical viscosity value η_c for glass transition in MGs. In fact, at T_g, the viscosity of various liquids get to $\eta(T_g) = 10^{13}$ poise,[1] which is independent of materials. This indicates that the yield is similar to the transition from glass state to its supercooled liquid state. When a MG is uniaxially compressed or stretched at RT and if the applied stress exceeds σ_c, x will increase to x_C, and the viscosity is then much decreased and the shear flow or the initiation and subsequent development of shear bands occurs in the MGs.

2. The characterization of the transition from MGs to supercooled liquids

Next, the features of the transition from MG to supercooled liquid in different MGs with markedly different physical and mechanical properties[14,16,19,20] (listed in Table II) are investigated. The value of steps of specific heat capacity (ΔC_p) during glass transition in a variety of MGs was determined as the temperature of intersection between the extrapolated lines of the glass C_p and the rapidly rising C_p during the glass transition, and the ΔC_p was the difference between the extrapolated C_p values of the supercooled liquid state and the glass state at T_g (see inset of Fig. 2).

The data of ΔC_p and T_g for 43 MGs are list in Table II and drawn in Fig. 2. One can see ΔC_p is around 12.9 (±1.0) J·mol^{-1}·K^{-1} and almost invariable for the different MGs. I note that some data of the specific heat difference between undercooled liquid and glass are different from that reported in Ref. 33. This is due to in Ref. 33, the data collected from different groups and different literatures from our group, there are systematical errors. In this paper, we then remeasured the data and to reduced the systematical errors. This is the reason why the present data have minor differences compared to that of Ref. 33.

It is noted that specific heat at T_g has been previously reported by other groups in vit1, Mg-Cu-Y, Pd-Ni-Cu-P bulk MGs.[38–42] They provided equations for the specific heat as a function of temperature.[38–42] Here, we only focus on the difference of C_p at T_g between glass and supercooled liquid states. When one carefully checks the difference of C_p in their work using our method, one can find that their results are actually similar to ours. The minor difference could result from effects of the thermal effects of the physical aging (overshoot) and the crystallization in undercooled liquid on the C_p measurement by DSC. According to Eyring's theory,[37] the invariable ΔC_p in MGs can be explained by the critical free volume change during the glass transition. The heat capacity of glass can be assumed to consist of two components, $C_{p\text{-}total} = C_{pv} - C_{ph}$. It is only the latter part that accounts for ΔC_p. As proposed by Eyring, C_{ph} is expressed as[37]

$$C_{ph} = \frac{RV_o}{V_h}\left(\frac{\varepsilon_h}{RT}\right)^2 e^{-\varepsilon_h/RT}, \quad (3)$$

where V_0 is the average atomic volume, V_h is the volume of a hole, and ϵ_h is the excess energy needed to form such a hole, and R is the gas constant. According to the Eyring's model,[37] $V_0/V_h \approx 5$ - 6 and $\epsilon_h/RT_g \approx -\ln x_c$. The RFV x is defined as the fraction of the total holes volume in the glass or liquid state. At T_g, the x is a critical value x_c. Taken $\Delta C_p = C_{ph} = 12.90$ J·mol^{-1}·K^{-1} and $V_0/V_h = 5$ during glass transition, we get the critical free volume x_c is 0.024. This indicates that the glass transition for MGs corresponds to the state where the fraction of the free volume reaches a critical value of 0.0238. The value is also very close to the above critical RFV value for the onset of yielding in MGs. That is, there is existence of a universal critical value of $x_C \sim 2.4\% \pm 0.2$ for both of the onset of glass transition and yield for various MGs. It is recently found that a universal

Author complimentary copy. Redistribution subject to AIP license or copyright, see http://jap.aip.org/jap/copyright.jsp

TABLE II. The composition, glass transition temperature Tg, and steps in heat capacity C_P of 45 kinds of MGs (Refs. 14, 19, 20, 33, and 45).

Name	Tg (K) (±2 K)	C_P ($JK^{-1}mol^{-1}$) (±1.5 $JK^{-1}mol^{-1}$)	Name	Tg (K) (±2 K)	C_P ($JK^{-1}mol^{-1}$) (±1.5 $JK^{-1}mol^{-1}$)
Ce68Al10Cu20Co2	351	12.6	Pr55Al25Co20	500	12.7
(La0.1Ce0.9)68Al10Cu20Co2	353	12.7	La55Al25Co20	526	13.4
(La0.2Ce0.8) 68Al10Cu20Co2	355	12.6	Nd55Al25Co20	541	12.8
(La0.3Ce0.7) 68Al10Cu20Co2	357	13.5	Pd40Ni40P20	570	13.7
(La0.4Ce0.6) 68Al10Cu20Co2	360	12.9	Pd40Cu30Ni10P20	571	13.7
(La0.5Ce0.5) 68Al10Cu20Co2	362	13.4	Sm40Y15Al25Co20	585	12.7
(La0.6Ce0.4) 68Al10Cu20Co2	362	12.5	Gd55Al25Co20	601	13.4
Au60Cu15.5Ag7.5Si17	365	12.9	Tb55Al25Co20	619	12.9
(La0.8Ce0.2) 68Al10Cu20Co2	366	13.1	Zr58.5Cu15.8Ni12.5Al10.3Nd7.8	630	12.7
(La0.7Ce0.3) 68Al10Cu20Co2	366	12.9	Dy55Al25Co20	632	12.8
(La0.9Ce0.1) 68Al10Cu20Co2	367	13.4	Y55Al25Co20	638	12.7
La 68Al10Cu20Co2	374	13.4	Zr46.75Ti8.25Cu7.5Ni10Be27.5	640	12.9
Ca65Mg15Zn20	375	13	Pd77.5Cu6Si16.5	640	12.7
Ce62Al10Cu20Co3Ni5	378	13.4	Zr65Al7.5Ni10Cu17.5	650	12.5
Zn40Mg11Ca31Yb18	400	13.2	Ho55Al25Co20	651	12.6
La62Al14Cu20Ag4	404	13.4	Zr65Cu15Ni10Al10	652	12.8
Mg65Cu25Tb10	413	13.5	Zr55Al10Ni5Cu30	682	12.8
Mg65Cu25Sm10	416	13.2	Zr55Cu25Ni10Al10	685	13.3
Mg65Cu25Gd10	417	13.3	Cu46Zr46Al7Gd1	700	12.9
Mg65Cu25Ho10	417	12.6	Cu46Zr46Al8	701	13.3
Mg65Cu25Y10	418	12.9	Zr50.7Cu28Ni9Al12.3	719	12.9
La57.6Al17.5Cu12.4Ni12.5	435	13.1	Zr44Cu44Al6Ag6	722	13.1
La55Al25Ni5Cu10Co5	455	12.8			

scaling law that uncovers an inherent relationship of yield strength τ_y with T_g of MGs.[43–46] All the results demonstrate that there is an intrinsic correlation between yielding and glass-liquid transition, and the yielding of MGs is intrinsically associated with the glass transition.

Some similar critical behaviors have been found in MGs. For example, a Lindemann-type criterion for glass transition in MGs has been reported.[16] It is also found that the glass transition occurs when the G decreases to 85% of the shear modulus at 0 K, that is, $G(T_g) = 0.85G(0\ \mathrm{K})$. The existence of a universal critical value of $x_C \sim 2.4\%$ for the onset of yield and glass transition for various MGs is consistent with the found critical behaviors and the Lindemann-type criterion. The formation of free volume in liquids or glasses is related to the limiting mean-root-square displacement of a kinetic unit (an atom or a group of atoms) from an equilibrium position. Thereby, the critical RFV during the glass transition in the MGs characterizes a critical atom displacement, above which the structure of the MG would be disintegrated. According to the harmonic Debye model, the mean-square thermal displacement is proportional to $T/m_a\theta_D{}^2$ (where m_a is the molar mass and θ_D is the Debye temperature). Owing to the critical atom displacement at T_g, the $T_g/m_a\theta_D{}^2$ should have a critical value for MGs.[16]

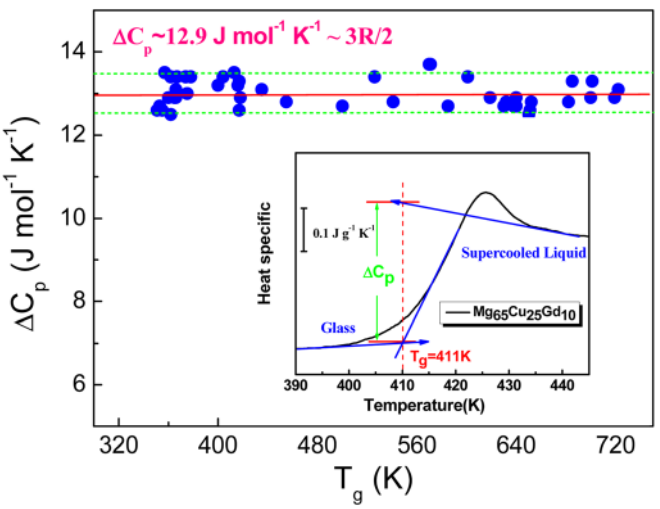

FIG. 2. (Color online) Plots of the glass transition temperature T_g and the excess specific heat of the various MGs listed in Table II. The inset shows how the difference of the specific heat is determined.

The results would be helpful for providing a simple picture for understanding the glass transition and yielding as a united issue. For MGs, the free volume was thought to be evenly distributed in the materials. The packing density around the free volume is lower than the surroundings. Therefore, these regions combine weakly and become the preferred sites where the MGs become instable caused by increasing temperature (glass transition) or applied stress (yielding) because both yielding and glass transition occurs when the reduced free volume evolutes to arrive at a similar critical value. Recent experimental observations and computer simulations indeed indicate that the yield point of MGs corresponds to the destabilized propagation by the percolation of a large number of local shearing events with a critical shear strain, γ_0.[11,16,17,47] The transition from local shearing events to macroscopic yield results from the dramatic increase of the atom mobility and softening motivated by the input of mechanical energy that could be both applied temperature or stress.[48,49] The yielding of MGs then can be

Author complimentary copy. Redistribution subject to AIP license or copyright, see http://jap.aip.org/jap/copyright.jsp

rationally presumed as a critical point at which the accumulated internal energy by elastic deformation is high enough for the transition from glass state to supercooled liquid state. It is suggested that one can unjam the jamming systems (the jammed systems include glass, grains, bubbles, droplets disordered systems) by raising temperature, applying a stress or decreasing the density.[50] Based on above experimental observations, it is proposed that temperature, stress, and decreasing density are equivalent approaches for fluidizing MGs.[51] The formation, deformation, and glass transition in MGs can be treated as the flow phenomenon.

3. Correlation between glass transition and plastic deformation in MGs

The underlying flow during glass transition is mainly governed by a kinetic process of the α-relaxation.[1–4] On the other hand, when an external stress beyond yielding strength is applied to MGs, the homogeneous or inhomogeneous flow (plastic deformation) occurs. Theories and models were often separately developed to understand the temperature induced flow associated with glass transition and the stress induced flow related with plastic deformation. Growing simulation and experimental evidences have suggested that glass transition and plastic deformation could be connected in MGs,[28,33,38,48,52] while more clear experimental evidences are needed to verify if there exists an intrinsic connection between the two fundamental issues in MGs. The effective activation energy of homogeneous plastic deformation and glass transition in various MGs are studied to check the connection between the two fundamental issues.

The deviation of α-relaxation from Arrhenius relation $\eta = \eta_\infty \exp(E_\alpha/\mathrm{RT})$ can be quantified by the fragility index m as[1]

$$m \equiv \left.\frac{\partial \log(\eta/\eta_\infty)}{\partial(T_g/T)}\right|_{T=T_g}, \tag{4}$$

where η_∞ is the high-temperature limit of viscosity, E_α effective activation energy of α-relaxation or glass transition. The dramatic slow down in η when temperature approaches T_g can be characterized by fragility. A pronounced non-Arrhenius liquids is characterized by large m value and called "fragile." While materials with small m values are "strong" glass, and their α-relaxation behaviors are close to the Arrhenius type. Metallic glasses with m value ranging about 30–60 belong to the intermediate fragile glasses.[16] If however, the Arrhenius relation is nevertheless used to depict the α-relaxation, the E_α must be temperature dependent, combination with Eq. (4), the E_α at T_g would be

$$E_\alpha(T_g) = mRT_g \ln(10). \tag{5}$$

The m dependent $E_\alpha(\mathrm{T_g})$ characterizes the maximum energy barrier a MG should overcome when heated from glass onward to supercooled liquid state. Intriguingly, in MGs, the m is found to correlate with the glass forming ability,[53] the behavior of the β-relaxation,[24,54] and the high frequency dynamics of atomic vibration (Boson peak).[55] Remarkably, the m is also recognized as the indicator of ductility of MGs.[14]

While at high temperature (>~0.8 T_g) and within the supercooled liquid region, MGs can be deformed either by non-Newtonian or Newtonian homogeneous deformation depending on the strain rate. Although the low temperature inhomogeneous deformation mechanisms of MGs are poorly understood, the homogeneous deformation is amenable to statistical modeling using the transition rate theory.[10] For example, in the framework of plastic deformation theory, the constitutive law for T and shear stress τ dependent shear strain rate $\dot{\gamma}$ is[10,11]

$$\dot{\gamma} = \alpha_0 \upsilon_0 \gamma_0 \exp\left(\frac{-Q}{kT}\right) \sinh\left(\frac{\tau V}{kT}\right), \tag{6}$$

where α_0 incorporates the fraction of material that is available to deform via activated process,[10] υ_0 attempt frequency of a flow unit on the order of Debye frequency, Q the activation energy, γ_0 the characteristic strain of a operated plastic unit, $V^* = \gamma_0 \Omega$ the activation volume with Ω the characteristic volume of a flow unit. Equation (6) is not theory specific[10,56] and other models such as STZ theory, free volume theory,[12] and Eyring's theory[26] also give the similar equations with different interpretations of the prefactors. For a specific T, the common expression of $\dot{\gamma}$ versus τ is $\dot{\gamma} = A \sinh(B\tau)$, where A and B are T dependent fitting parameters, $A = \alpha_0 \nu_0 \gamma_0 \exp(-Q/kT)$ and $B = V^*/kT$. Assuming α_0 is T independent, then the plot of ln(A) versus $1/T$ of the data gives Q values.

Figure 3(a) shows compressive strain rate-stress-temperature deformation diagram for a $Zr_{41.2}Ti_{13.8}Cu_{12.5}Ni_{10}Be_{22.5}$ (vit1, $T_g \sim 613$ K) MG (Refs. 10 and 56) over a broad range of temperature [from 517 K (far below its T_g) to its supercooled liquid region]. The relation $\sigma = \sqrt{3}\tau$ is used,[10] where σ is compressive stress. Figure 3(b) shows a plot of $ln(A)$ versus T_g/T for vit1 in the T range from glass state to supercooled liquid state and gives $Q \approx 490 \pm 20$ kJ/mol $\approx 97RT_g$. The activation volume is estimated to be $V^* \approx 95 \pm 15$ Å^3. The Q and V values are consistent with the results of Schuh *et al.* ($Q \sim 4.6$ eV or 445 kJ/mol, and $V^* \tilde{}\, 75$ Å^3),[10] and the values are almost T independent. Furthermore, the value of $Q/RT_g ln(10) \approx 42 \pm 3$ is very close to the fragility index of vit1, $m \approx 45 \pm 5$ (kinetic $m = 50$ and thermodynamic $m = 39$).[17] This result implies that the activation energy of homogeneous deformation in vit1 is equivalent with its effective activation energy of α-relaxation at T_g, that is

$$Q \approx E_\alpha(T_g). \tag{7}$$

To investigate whether Eq. (7) stands in other MG systems, we collect the available data of Q and m from literatures[56–63] for different MGs and estimate their $E_\alpha(T_g)$ using Eq. (5). All the available data are listed in Table III. Figure 4 shows a plot of Q versus $E_\alpha(T_g)$ for various MGs. Clearly, the data reveal nearly a one-to-one correspondence between Q and $E_\alpha(T_g)$ that extends over a broad range. A least square linear fit gives a correlation coefficient about 0.93 and the slope of the fitted line is about 1.4 ± 0.3. This suggests a clear correlation between Q and $E_\alpha(T_g)$ and the validity of Eq. (7). The above result is not unexpected, since homogeneous deformation is often regarded as a process of balancing between

Author complimentary copy. Redistribution subject to AIP license or copyright, see http://jap.aip.org/jap/copyright.jsp

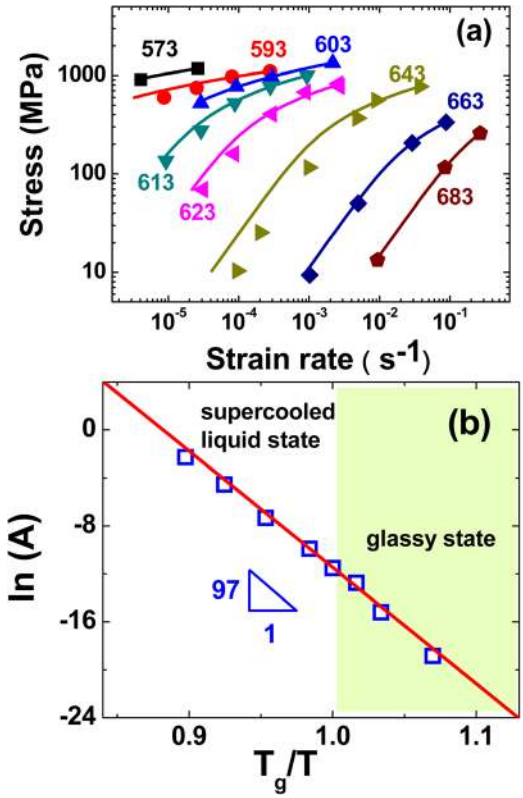

FIG. 3. (Color online) (a) The strain rate-stress-temperature diagram for $Zr_{41.2}Ti_{13.8}Cu_{12.5}Ni_{10}Be_{22.5}$ (vit1, $T_g \sim 613$ K) MG (Ref. 51), the solid curves are fitted in the form $\dot{\gamma} = A\sinh(B\sigma)$ where $\sigma = \sqrt{3}\tau$ is the compressive stress (Ref. 10). From the fitting, A and B can be determined. (b) Arrhenius plot of ln(A) vs T_g/T for vit1. The solid line is a least square linear fit.

stresses driven free volume creation and relaxation induced free volume annihilation.[10] From the energy landscape perspective, the Newtonian homogeneous deformation is regarded as thermally activated flow, where energy barriers are overcome entirely by thermal fluctuations.[28,43,52,63] Besides, in the high temperature and low stress limit $\dot{\sigma}_{flow} = 3\eta$, mechanical experiments and viscosity measurements are equivalent in determining the activation energy. Under this condition, Eq. (7) should strictly hold. The correlation between plastic deformation and α-relaxation via activation energy unequivocally demonstrates the similarity between the plastic deformation and thermally driven glass transition. Very recently, a new bulk MG that has very low elastic modulus ($G = 6$ GPa) was developed.[64] Due to the low flow activation energy of the MG, the glass transition or homogenous flow can be realized by applied stress at RT, which confirms the similarity of plastic flow and glass transition in MGs.

TABLE III. Data about the activation energy of steady state homogeneous deformation Q, glass transition temperature Tg, fragility index m, and estimated effective activation energy of α-relaxation E_α for typical MGs (Refs. 56–62).

MG	Q (kJ/mol)	Tg (K)	m (±5)	E_α(Tg) (kJ/mol)
Zr41.2Ti13.8Cu 12.5Ni10Be22.5	445	613	45	492
Zr52.5Al10Cu22Ti2.5Ni13	521	659	40	505
Pd41Ni10Cu29P20	871	576	60	662
Mg65Cu25Y10	277	425	35	285
Zr55Cu30Al10Ni5	405	678	35	454
Zr49Cu46Al5	660	694	45	598
Cu47.5Zr47.5Al5	654	702	45	605
Zr65Cu15Al10Ni0	375	652	30	374
Pd40Ni40P20	665	597	50	571
La55Al25Ni20	267	479	40	362
Ce70Al10Cu20	130	366	28	195

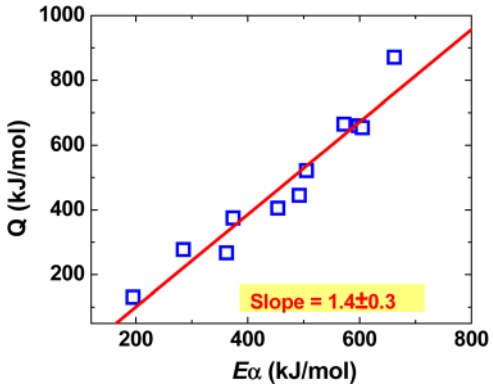

FIG. 4. (Color online) Relationship between activation energy Q of steady state homogeneous deformation and effective energy barriers E_α of α-relaxation.

B. Correlation between the activation of plastic events and β-relaxations in MGs

In microscopic scale, the plastic deformation of MGs is accommodated by a consequence of formations plastic events involved in the rearrangement of tens of atoms and self-organizations of the plastic events. The plastic event is modeled as shear transformation zone, STZ,[11] and the STZs are regarded as the microscopic unit event of shear banding and yielding. The slow β-relaxation[3] is usually related to localized motions with cooperative nature, a reminiscent of STZs in MGs and is the microscopic unit event leading to primary α-relaxation. The activation energy of the β-relaxations of MGs E_β is experimentally determined either by DSC or by DMS.[23,24,65] Next, the correlation between the microscopic unit event of shear banding and yielding (plastic units) and the microscopic unit event leading to primary α-relaxation (the slow β-relaxation) in MGs is investigated.

The DMS measurements were performed on MGs with varied testing frequency f. Table IV summarizes available data of E_β and T_g for various MGs,[23,24,54,66] which covers more than 20 individuals from 10 typical MG systems. Figure 5(a) shows the plot of E_β against RT_g of these MGs. An approximately linear relationship of $E_\beta \approx 26(\pm 2)RT_g$ is obtained. The similar empirical relationship between E_β and T_g in the form of $E_\beta \approx 24RT_g$ had also been found in nonmetallic glasses.[11]

The potential energy barrier for an unsheared STZ can be estimated as:[13] $W = (8/\pi^2)G\gamma_c{}^2\zeta\Omega$, where Ω the average volume of an STZ, $\gamma_c \approx 0.027$ the average elastic limit, and $\zeta \approx 3$ a correction factor arising from the matrix confinement of a "stressed" STZ.[13,49] Let $\Omega = nC_fV_a$, where $V_a = M/(\rho N_0)$ the atomic volume, N_0 Avogadro's number, r density, and M

Author complimentary copy. Redistribution subject to AIP license or copyright, see http://jap.aip.org/jap/copyright.jsp

TABLE IV. Activation energy of β relaxation E_β, Tg, of different metallic glasses. In DMS, the Tg was determined at the testing frequency of 1 Hz (Refs. 23, 24 and 66).

Metallic glass	E_β (kJ/mol)	Tg (K)	Method
La70Ni15Al15	93	441	DMS
La60Ni15Al25	100	475	DMS
La50Ni15Al35	110	534	DMS
La55Al15Ni10Cu10Co10	89	446	DMS
Cu47Zr47Al6	155	700	DMS
Cu45Zr45Al10	153	703	DMS
Zr46.75Ti8.25Cu7.5Ni10Be27.5	118	648	DMS
Zr64.13Cu15.75Ni10.12Al10	112	646	DMS
Zr57Cu15.4Ni12.6Al10Nb5	135	663	DMS
Tm39Y16Al25Co20	151	657	DMS
La55Al25Ni20	110	493	DSC
Pd40Ni10Cu30P20	129	575	DMS
Zr46.75Ti8.25Cu7.5Ni10Be27.5	138	628	DMS
Zr65Cu15Ni10Al10	131	654	DMS
(Cu50Zr50)92Al8	174	692	DMS
La57.5(Cu50Ni50)25Al17.5	92	435	DMS
(Fe85Ni15)83P17	134	650	DSC
(Fe85Cr15)83P17	150	720	DSC
(Fe85V15)83P17	162	728	DSC
(Fe85Mo15)83P17	189	754	DSC
(Fe75Ni25)83P17	111	640	DSC
(Fe75Co25)83P17	146	685	DSC
(Fe75Mn25)83P17	141	697	DSC
(Fe75Cr25)83P17	166	765	DSC
(Fe50Ni50)83B17	172	650	DSC
(Fe5Ni5)83P17	154	645	DSC
Pd48Ni32P20	92	582	DSC
Al82Ni10Ce8	158	585	DSC
Pd43Ni10Cu27P20	106	568	DMS

molar mass, $C_f \sim 1-2$, as suggested by Falk *et al.*,[15] is a free volume parameter. The n is estimated to be about ~100 - 300 [Refs. 13 and 17]. The molar potential energy barrier for an unsheared STZ is

$$W_{STZ} = N_0 W = \left(\frac{8}{\pi^2}\right) n G \gamma_c^2 \zeta C_f V_m, \tag{8}$$

where $V_m = N_0 V_a$ is the molar volume. Taking $C_f = 1.12$, $n = 200$, we get: $W_{STZ} \approx 0.397 G V_m$. The relevant data of G, V_a, and GV_m and estimated W_{STZ} for more than 40 different MGs are collected in Table V.[16,17,20,28,45,67–74]

Figure 5(b) exhibits a plot of the W_{STZ} versus the E_β for the MGs listed in Table V. The data reveal nearly a one-to-one correspondence between E_β and W_{STZ} that extends over a broad range of MGs. The least square linear fitting line (with a correlation coefficient about 0.90) roughly passes though the point of origin with a slope of 0.99 ± 0.08, which confirms that $E_\beta \approx W_{STZ}$. This linear relationship is further verified to hold in individual system of MGs with varying of composition (such as Zr-, Cu-, Fe-, and rare-earth based MGs).[28,71] Therefore, the above results confirm that activation of STZs and the β-relaxations are directly correlated. As GV_m is a measurement of the energy barrier of STZs and RT_g measures the activation energy of the β-relaxation, one can readily use GV_m and RT_g, which are easily measurable parameters, to characterize the events of STZs and the β-relaxations in MGs.

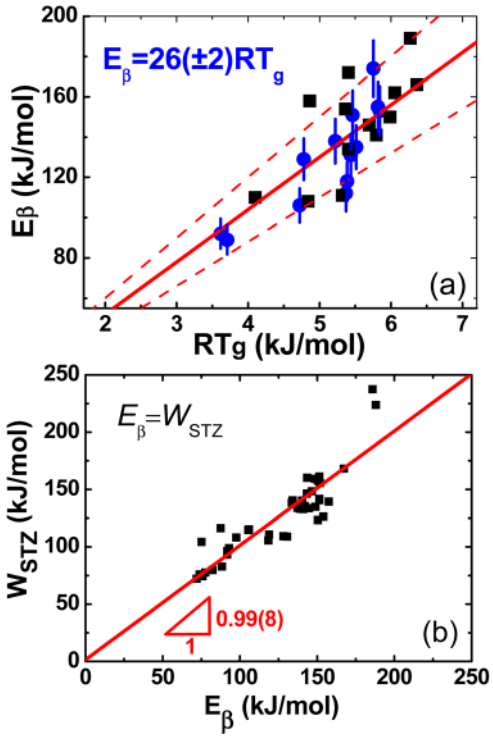

FIG. 5. (Color online) (a) Relationship between activation energy of β-relaxation E_β and RT_g for MGs listed in Table IV (Ref. 28).The squares and circles denote measurements from DSC and DMS, respectively. The solid line is a least square linear fit; (b) Relationship between activation energy of β-relaxation E_β and energy barriers of STZs, W_{STZ} (Ref. 28).

This generalized correlation in essence is a manifestation of the close relationship between activation of STZs and β-relaxation.[28] It is believed that the β-relaxation relates to the dynamical heterogeneity in glasses.[1,3] On the other hand, there is general consensus that the potential STZs are nucleated around the sites of free volumes.[1–3] This picture is validated by the experimental observations that some bulk MGs consist of the weakly bonded regions (or soft regions) and strongly bonded regions (or hard regions)[74–76] and the heterogeneous structure benefit the plastic deformation of these MGs. Therefore, the β-relaxations, similar to the events of potential STZs, could take place in the loosely packed regions, where the local translational atomic motions can be readily activated compared with that in closely packed regions, and the structural heterogeneity is the common structural origin of events of STZs and the β-relaxations. The β-relaxation in MGs then corresponds to a process involving "thermal driven events of STZs," i.e., a group of atoms within loosely packed regions undergo an inelastic distortion from one configuration to another, crossing an energy barrier induced by the thermal fluctuations, and there is no directional flow and the process is reversible due to the confinements of the surrounding closely packed regions. In contrast, the directional flow events of STZs are induced by external shear stress.[28] Therefore, in microscopic scale, the plastic flow unit of MGs is closely related to the unit event of the relaxation, the β-relaxation.

Author complimentary copy. Redistribution subject to AIP license or copyright, see http://jap.aip.org/jap/copyright.jsp

TABLE V. The data of density ρ, atomic volume Va, G, ν, Tg, GVm, and W_{STZ} for MGs (Refs. 16, 17, 20, 28, 44 and 67–73).

MG	ρ (g/cm^3)	Va (Å^3)	G (GPa)	GVm (kJ/mol)	v	Tg (K)	W_{STZ} (kJ/mol)
Au49Ag5.5Pd2.3Cu26.9Si16.3	11.60	18.27	26.5	291.4	0.406	405	115.7
Au55Cu25Si20	12.20	17.68	24.6	261.8	0.417	348	103.9
Ca65Li9.96Mg8.54Zn16.5	1.96	33.64	9.0	180.9	0.307	333	71.8
Ce68Al10Cu20Co2	6.81	27.30	11.4	186.6	0.333	351	74.1
Ce70Al10Cu20	6.70	28.14	11.3	190.6	0.329	342	75.7
Ce70Al10Ni10Cu10	6.67	28.14	11.5	194.8	0.313	359	77.3
Cu46Zr42Al7Y5	7.23	16.97	31.0	316.8	0.364	713	125.8
Cu46Zr46Al8	7.08	17.22	34.3	355.4	0.366	701	141.1
Cu46Zr54	7.62	17.11	30.0	309.0	0.391	696	122.7
Cu48Zr48Al4	7.22	17.34	32.4	338.2	0.370	689	134.3
Cu50Hf43Al7	11.00	16.67	42.0	421.6	0.358	774	167.4
Cu50Zr50	7.40	17.36	32.0	334.7	0.360	670	132.9
Cu57.5Hf27.5Ti15	9.91	15.56	37.3	349.3	0.356	729	138.7
Dy55Al25Co20	7.56	23.71	23.5	335.7	0.304	635	133.3
Er55Al25Co20	8.16	22.51	27.1	366.8	0.306	663	145.6
Fe53Cr15Mo14Er1C15B6	6.92	13.19	75.0	595.6	0.320	860	236.5
Fe61Mn10Cr4Mo6Er1C15B6	6.89	12.42	75.0	560.8	0.280	870	222.6
Fe68Mo5Ni5Cr2P12.5C5B2.5	7.50	11.41	57.9	397.8	0.329	699	157.9
Fe70Mo5Ni5P12.5C5B2.5	7.48	11.45	57.3	395.1	0.331	696	156.9
Fe74.5Mo5.5P12.5C5B2.5	7.54	11.38	56.9	389.9	0.326	702	154.8
Ho55Al25Co20	7.89	23.01	25.4	351.7	0.311	649	139.6
La55Al25Cu10Ni5Co5	6.00	26.41	15.6	248.0	0.342	430	98.5
Lu39Y16Al25Co20	7.59	22.09	30.0	399.2	0.316	687	158.5
Lu55Al25Co20	8.69	21.93	30.6	404.1	0.307	701	160.4
Mg65Cu25Gd10	3.79	20.78	19.3	241.4	0.313	425	95.8
Mg65Cu25Y10	3.28	20.53	18.9	233.8	0.329	425	92.8
Pd40Cu30Ni10P20	9.28	13.19	34.5	274.0	0.399	593	108.8
Pd40Cu40P20	9.30	13.25	33.2	264.8	0.402	548	105.1
Pd64Ni16P20	10.10	13.76	32.7	271.0	0.405	452	107.6
Pd77.5Cu6Si16.5	10.40	14.52	31.8	278.0	0.409	550	110.4
Pr60Al10Ni10Cu20	6.88	25.57	13.5	207.6	0.300	409	82.4
Pt57.5Cu14.7Ni5P22.8	15.20	14.37	33.4	289.0	0.434	490	114.7
Pt60Ni15P25	15.70	14.14	33.8	287.6	0.420	488	114.2
Tm39Y16Al25Co20	7.30	22.44	29.7	401.3	0.304	664	159.3
Yb62.5Zn15Mg17.5Cu5	6.52	31.97	10.4	200.0	0.276	381	79.4
Zr41.2Ti13.8Ni10Cu12.5Be22.5	5.90	16.90	34.1	347.0	0.352	618	137.8
Zr46.75Ti8.25Cu7.5Ni10Be27.5	6.00	16.53	35.3	351.3	0.355	621	139.5
Zr48Nb8Ni12Cu14Be18	6.70	17.05	34.3	352.1	0.367	620	139.8
Zr62Cu15.5Ni12.5Al10	6.62	19.20	28.9	333.6	0.378	643	132.4
Zr64.13Cu13.5Ni12.37Al10	6.65	19.25	28.9	332.7	0.377	652	132.1

C. The flow in metallic glasses and metallic glass-forming liquids

In this section, we focus on the definition of the flow and characterize the flow in MGs and MG-forming liquids. A viscous liquids can be viewed as "solid that flows" in enough short time scale.[7,72] Figure 6 schematically illustrates the flow based on the concept of potential energy landscape (PEL). The flow event or the configurational hopping in MGs or MG-forming liquids is the process that the system escapes from one local minimum to another (an activated hopping between inherent states across energy barrier ΔE) or the disappearance of barrier between neighbor local minima. There are two flow modes: the β-mode is the stochastically and reversible activated hopping events across ''sub-basins'' confined within the inherent ''megabasin'' (intrabasin hopping) and the α-mode is irreversible hopping events extending across different megabasins (interbasin hopping). Figure 6 also schematically illustrates the relationships among the potential plastic units, plastic flow or yielding, and the β- and α-relaxations, based on the PEL in MGs.[4] The isolated potential STZs accommodating the flow during glass transition or plastic deformation are confined within the elastic matrix and correspond to the β-relaxation. The mechanical stress, equivalent to thermal activation, can significantly enhance the atomic mobility (or decrease the viscosity) by inducing a glass-to-supercooled-liquid transition. When temperature or external stress is applied and reaches a critical energy threshold of activation energy for the transition from MG to a supercooled liquid with high atom mobility, the elastic shell of the isolated STZs will collapse, and the percolation of these flow units associates with the α-relaxation. The localized plastic deformation or shear banding in MGs

Author complimentary copy. Redistribution subject to AIP license or copyright, see http://jap.aip.org/jap/copyright.jsp

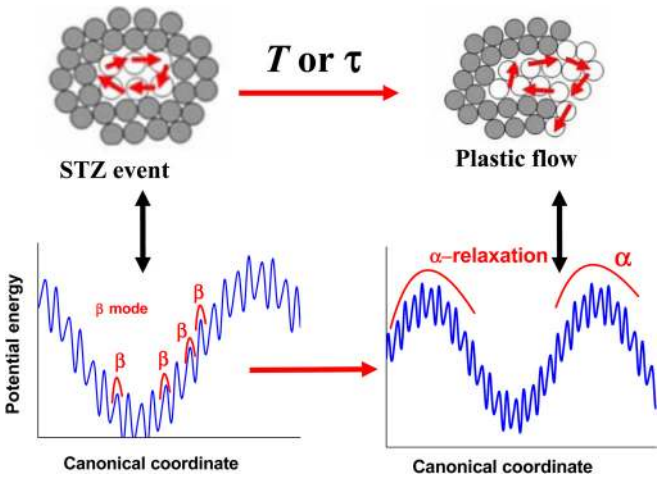

FIG. 6. (Color online) Above: A 2D schematically illustration of STZ activation (top left panel), α-relaxation (flow and yielding, top right panel), and their corresponding origination of potential energy landscapes (bottom panel). Filled circles represent atoms with low propensity of motion, while open circles represent atoms with high propensity of motion. The arrows indicate the possible motion of atoms. The potential STZ events are localized with cooperative nature and is reversible due to confinements of surrounding materials, while α-relaxation (percolation of STZs, or plastic flow and yielding) incorporates large scale atomic migration and irreversible. Below: A schematically illustration of flow and its corresponding origination of potential energy landscapes. There are two kinds of flow modes: the β-mode is the stochastically and reversible activated hopping events across ''sub-basins'' confined within the inherent ''megabasin'' (intrabasin hopping) and the α mode is irreversible hopping events extending across different landscape megabasins (interbasin hopping).

can be regarded as the percolation of these flow units in nano-scale thin layers (shear bands) driven by stress, and the glass transition or α-relaxation is a thermally driven large scale percolation of these flow units in whole material. The plastic deformation, glass formation, glass transition, and relaxations in MGs can be treated as the flow phenomenon activated by different processes such as thermal process or mechanical process. The flow is controlled by its activation energy. Next, the physical parameters that the flow activation energy related to will be investigated.

D. An elastic model for flow in MGs and MG-forming liquids

The MG-forming liquids can be characterized by the instantaneous elastic moduli of G_∞, E_∞, and K_∞. Actually, the metallic glasses are frozen liquids and their atoms or clusters are arranged much like those in their melt but are more tightly, densely packed, and much more viscous. It is found that even below the conventional elastic limit, the MGs show nonelastic rheological response under constant load.[35] In accordance with the properties, the MGs can be characterized as highly viscousic. Extensive experimental evidence shows that the flow viscosity of MG-forming liquids follows the general Arrhenius equation: $\eta(T) = \eta_0 \ln[\Delta E(T)/k_B T]$. The energy barrier ΔE for the flow events is temperature dependent and can be determined based on the PEL theory.

We define the activation energy of a unit volume as the activation energy density (ρ_E) (Refs. 77–82):

$$\rho_E = \frac{\Delta E}{V_m}. \tag{9}$$

The definition of activation energy density can directly relate the flow activation event to the elastic moduli.[7,8,18,81,82]

We estimate the energy barrier between two potential energy minima from the curvature around the minima.[18,82] Consider the one-dimensional PEL with two minima separated the distance $2r_0$ as shown in Fig. 7. The two thin curves give the potential estimated by second-order expansions around the minima, and the barrier height is estimated by extrapolating from the minima. The estimated barriers are clearly larger than the actual barriers as shown in Fig. 7, but the estimated and actual barriers are proportional. The activation energy ΔE for flow in MGs or in MG-forming liquids is assumed to be mainly elastic energy.[7,64] Then, in the energy landscape perspective, the activation energy density of flow can be expressed in a harmonic form $\rho_E = \frac{1}{2}Mr^2$ using second order Taylor expansion around the minima,[18] where M is the elastic moduli, and r is the elastic strain. According to the equipartition law of statistical mechanics: $\frac{1}{2}M\langle r^2\rangle \propto \frac{1}{2}k_B T/V_m$,[83] suggesting $\langle r^2\rangle \propto k_B T/MV_m$. Assuming the distance r_0 between the minima is constant, then,

$$\rho_E = \frac{1}{2}Mr_0^2 = \frac{1}{2}\frac{k_B T}{\langle r^2\rangle V_m}r_0^2, \quad \text{or} \quad \rho_E \propto \frac{k_B T}{\langle r^2\rangle V_m}.$$

Because the atoms release 3 degrees of freedom around glass transition in MGs,[33] one gets

$$\langle r^2\rangle V_m = \frac{k_B T}{M_x} + \frac{k_B T}{M_y} + \frac{k_B T}{M_z},$$

where x, y, z represent the three directions in Cartesian coordinate, and M_x, M_y, and M_z are the corresponding elastic moduli. For isotropic MGs, they represent two shear modulus and one longitudinal modulus, as $M_x = M_y = \rho v_s^2$ and $M_z = \rho v_l^2 = K + 4\,G/3$, where ρ is the mass density, and v_s and v_l are the shear and longitudinal sound velocities, respectively. Then, one gets

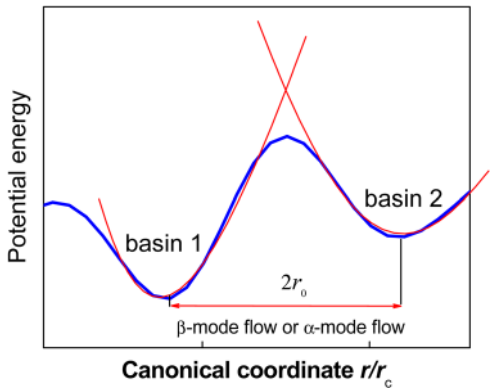

FIG. 7. (Color online) The schematic map of potential energy density landscape with the distance $2r_0$ between the minima. The thin curve gives the estimation by second order Taylor expansions around the minima. The barrier height estimated by extrapolating from the minima. The estimated and actual barriers are proportional.

Author complimentary copy. Redistribution subject to AIP license or copyright, see http://jap.aip.org/jap/copyright.jsp

$$\langle r^2\rangle V_m \propto \frac{2k_BT}{\rho v_s^2} + \frac{k_BT}{\rho v_l^2} = \frac{2k_BT}{G} + \frac{k_BT}{K+4G/3}. \quad (10)$$

And then, one obtains

$$\rho_E \propto \frac{G(K+4G/3)}{2K+11G/3}. \quad (11)$$

The linear contribution of G and K can be estimated by defining the temperature dependency of

$$\rho_E, I = \frac{d\ln\rho_E(T)}{d\ln T},$$

[Ref. 18]. That is

$$I = \left(1 - \frac{KG}{2K^2 + \frac{19}{3}KG + \frac{44}{9}G^2}\right) \bullet I_G + \frac{KG}{2K^2 + \frac{19}{3}KG + \frac{44}{9}G^2} \bullet I_K, \quad (12)$$

alternatively, $I = (1-\alpha) \bullet I_G + \alpha \bullet I_K$, where I_G and I_K are temperature indices,[18] respectively. And

$$\alpha = \frac{KG}{2K^2 + \frac{19}{3}KG + \frac{44}{9}G^2}. \quad (13)$$

For MGs, G/K varies from 0.2 to 0.5 [Ref. 16] and gives the partition coefficient of $\alpha = 0.07 \pm 0.01$. The partition coefficient for G and K suggests that both the volume-conservative shearing (corresponding to G) and volume-nonconservative dilatation (corresponding to K) contribute to the flow, and dilatation contributes around 7% to the activation energy density for creating the room for atoms rearrangement, which has been observed both by simulation and experiments.[11,84,85]

To determine exact contribution of K and G to the ρ_E for flow, the acoustic velocities change during glass transition has been studied. The T-dependent transversal and longitudinal velocities change differently during the glass transition process,[86] and the ratio of the relative changes of the two velocities is about

$$\frac{\Delta v_s}{v_s} : \frac{\Delta v_l}{v_l} \approx 2:1,$$

(Refs. 7 and 86). From $\rho v_s^2 = G$ and $\rho v_l^2 = \frac{4}{3}G + K$, we obtain the relative changes of G and K, $\frac{\Delta G}{G} : \frac{\Delta K}{K} \approx 5:1$. In $3D$ space, there are two shear modes (corresponding to G) and one radial mode (dilatation mode corresponding to K) when atoms move. Thus, the contribution of G should be doubled, and the ratio of the contribution of G and K in ρ_E should be about 10:1, that is

$$\rho_E = (10G + K)/11. \quad (14)$$

This indicates $\alpha = 1/11 = 9\%$, which is consistent with the above result.

The extended elastic model shows that ρ_E is determined by both G and K in a way of $\rho_E = (10G+K)/11$. This is different from most other elastic models for flow in glasses and supercooled liquids, which consider the case of simple shear and involve only shear modulus. The extended elastic model suggests that both homogeneous and inhomogeneous flow is shearing process combining free volume generation and demonstrates that both shear and free volume are important for flow and provides an intuitional picture of the flow of the atoms or atomic groups in glass or liquid. In fact, the shear induced dilatation has been widely observed.[84,85,87,88]

The elastic model is further experimentally verified. We check the correlations between T_g and the elastic moduli for various MGs. The flow viscosity of MG-forming liquids follows:

$$\eta(T) = \eta_0 \ln\left(\frac{\Delta E(T)}{k_BT}\right).$$

According to the definition of glass transition temperature, at T_g, for MGs, $\eta(T_g) = 10^{13}$ Pa·s.[1,4] From

$$\eta(T_g) = \eta_0\left(\frac{\Delta E(T)}{kT_g}\right) = 10^{13}\text{Pa} \times \text{s},$$

or

$$\frac{\Delta E(T)}{RT}\Big|_{T=T_g} \equiv \text{constant}.$$

One can see that $\Delta E(T_g)/kT_g$ is a constant at T_g for all MGs. According to our model,

$$\frac{\rho_E V_m}{RT_g} = (10G+K)V_m/11RT_g = \text{constant}.$$

Figure 8(a) shows the data of $(10G+K)V_m/11RT_g$ versus various kinds of MGs. These MGs cover many typical systems including Zr-, Cu-, Ca-, Mg-, Ni-, Fe-, and rare earth elements based MGs, and their thermal, mechanical, and physical properties are markedly different[17,80,81] (as listed in Table VI). Their values of T_g, E and Poisson's ratio span from 317 K to 930 K, 23 GPa to 195 GPa, 0.276 to 0.41, respectively. One can see that these data can be well fitted by a constant 0.075. The data of $(10G+K)V_m/11RT_g$ for various MGs versus other parameters such as density and Poisson's ratio are shown in Fig. 8(b). The MGs are independent with these parameters and can also be well fitted by the constant of 0.075. The experimental comparison further testifies the above model. As a comparison, Figs. 8(c) and 8(d) also show the plots of KV_m/T_g and GV_m/T_g versus Poisson's ratio. Fitting to the data yields $KV_m/T_g \propto 8.78\,v$ and $GV_m/T_g \propto -0.86\,v$, which indicate that the sole K or G cannot characterize the activation energy density well. Other groups[43,44,89,90] also found similar correlations in different forms, while these correlations also support that the volume factor must be considered to make the ratio of activation energies and T_g be a constant.

To further experimentally confirm the elastic model in glass state, an attempt was made to amplify the measurable dilatation effects of homogeneous deformation by performing tests at RT to suppress structural relaxation.[87] According to the elastic model, it is expected that plastic deformation induces dilatation of the glassy structure. In inhomogeneously deformed samples, the shear bands show clear structural changes resulting from the very high local shear, and

Author complimentary copy. Redistribution subject to AIP license or copyright, see http://jap.aip.org/jap/copyright.jsp

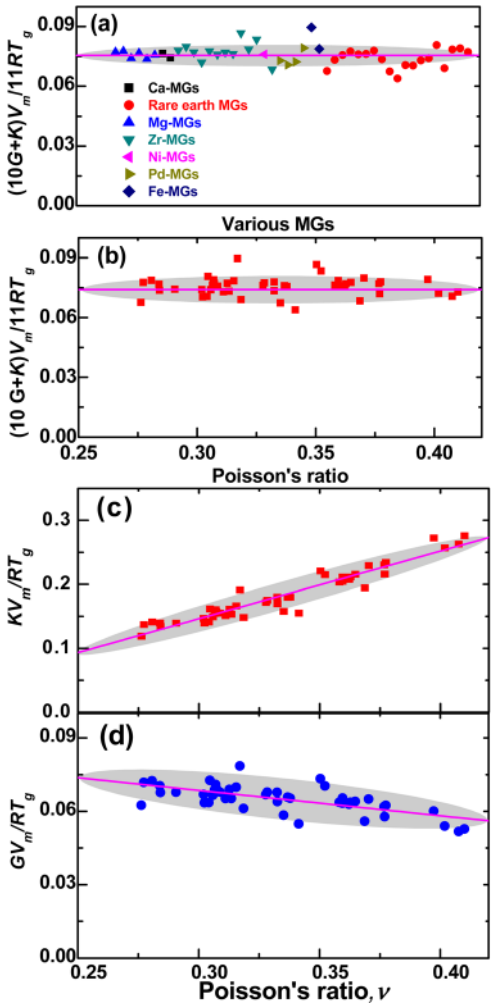

FIG. 8. (Color online) (a) The experiment data of $(10G+K)V_m/11RT_g$ vs various MGs. (b) The $(10G+K)V_m/11RT_g$ vs ν. The $(10G+K)V_m/11RT_g$ is independent of MGs and can be well fitted by a constant. (c) The KV_m/RT_g and (d) GV_m/RT_g vs ν for the same MGs. The fit result shows they have clear dependence on ν (Ref. 82).

possibly also linked to local heating and rapid cooling.[91,92] The $Zr_{46.75}Ti_{8.25}Cu_{7.5}Ni_{10}Be_{27.5}$ (vit 4, $T_g = 625$ K) is chosen to perform tests below its yielding strength at RT to suppress structural relaxation. Ultrasonic measurements have been exploited to measure the subtle changes in the moduli of the MG uniaxially loaded with a strain rate of $1 \times 10^{-4}s^{-1}$ at 80% of the MG yield strength ($\sigma_y \approx 1.9$GPa) for periods of hours at RT. After 38 h of pre-compression, detectable permanent deformation after the load is removed is found. No shear bands are observed indicating the homogeneous deformation.[87]

The evolution of density and elastic moduli with pre-compression time within the apparently elastic region indicates that the pre-compression induces dilatation.[87] The relative variations of elastic moduli show that the E and G decrease by similar small amounts, while the K decreases slightly more.[87] Loading for 38 h, the viscous strain is $\sim 2 \times 10^{-4}$, associated with a fractional density decrease of $\sim 2 \times 10^{-3}$. The density change though large, ten times the viscous strain, is broadly consistent with the observed fractional decreases in elastic moduli of $(5 \text{ to } 7) \times 10^{-3}$. The decreases in K therefore appear entirely consistent with the dilatation induced by pre-compression.[87] It is noted that the elastic moduli and density increase during relaxation, and the increases are greater under hydrostatic pressure.[93,94] Therefore, the changes in elastic moduli and density in our case are not consistent with structural relaxation. Also, on annealing-induced relaxation,[95] the changes in K are much smaller than the changes in G or E, in contrast to the relative magnitudes in our case.

The above results suggest that free volume can be generated very effectively in homogeneous flow as in soils, granular media in general,[96,97] and in the deformation of MGs.[87,98] The found clear dilatation effect in the viscous flow in the apparently elastic regime of the glass reveals that the large volume increase association with the local shearing events.[87] This also indicates that the role of bulk modulus during flow. The results as well as others[88] further confirm the proposed elastic model.

E. Elastic perspectives on metallic glasses and MG-forming liquids

The systematically elastic property studies of various MGs show that the subtle microstructural changes induced by tuning composition, temperature, pressure, aging, and internal or external stress can be effectively characterized by the elastic moduli. In other words, there exist close links between the microstructural change and properties/features of the MGs through the medium of elastic constants.[16,94,99–104] On the other hand, there exists clear correlations in empirical levels among the elastic moduli, the glass formation and transition, the properties and features, and the strong/fragile characteristics of MGs.[13,14,16,17,44,45,71,105,106] These correlations confirm that the elastic moduli are key parameters for controlling the features and properties of MGs. The elastic model in turn can offer a simple scenario for explaining and understanding the nature and characteristics of metallic glasses and the found correlations in MGs.[16]

For example, elastic model can explain the found critical phenomena during glass transition and yield. For MGs, it is found that the glass transition occurs when the G decreases to 85% of the shear modulus at 0 K, $G(T_g) = 0.85G(0 \text{ K})$.[107] According to the elastic model, the glass transition can be regarded as a kind of dramatic elastic moduli change caused by either temperature (glass transition) or densification (jamming) or load (external stress). These factors play similar roles in glass transition through rapidly changing the elastic moduli at glass transition point. In MG-forming liquids, when the temperature is rapidly cooled to T_g, the elastic moduli will rapidly reach the elastic moduli softening line, and the liquid is frozen into glass. One can also unfreeze the glass or yield the glass and make glass flow either by raising temperature or by applying shear stress to reach the elastic moduli softening line. The plastic deformation in MGs can also regarded as the glass to supercooled liquid transition (confined in shear bands), which occurs upon reaching an elastic modulus threshold by stress to sufficiently high internal energy.

The various correlations found in MGs can be understood via the elastic model. According to the framework of

Author complimentary copy. Redistribution subject to AIP license or copyright, see http://jap.aip.org/jap/copyright.jsp

TABLE VI. The Tg, average molar volume Vm, ν, and the combined parameters Moduli·Vm/RTg of 46 different kinds of MGs (Refs. 16, 79, and 80).

Compositions	Tg (K)	Vm cm^3/mol	υ	GVm/RTg	KVm/RTg	(10G + K)11Vm/RTg
Ca65Mg8.54Li9.96Zn16.5	317	20.25	0.307	0.0688	0.155	0.0765
Ca65Mg8.31Li9.69Zn17	320	20.10	0.291	0.0678	0.139	0.0743
Yb62.5Zn15Mg17.5Cu5	385	19.24	0.276	0.0625	0.119	0.0676
Ce70Al10Ni10Cu10	359	16.94	0.314	0.0653	0.153	0.0732
(Ce20La80)68Al10Cu20Co2	366	16.78	0.338	0.0654	0.180	0.0757
Ce68Al10Cu20Nb2	345	16.70	0.328	0.0678	0.175	0.0775
(Ce80La20)68Al10Cu20Co2	355	16.69	0.337	0.0658	0.180	0.0760
Ce68Al10Cu20Co2	352	16.57	0.328	0.0668	0.172	0.0763
Ce68Al10Cu20Ni2	352	16.57	0.333	0.0678	0.180	0.0779
Ce68Al10Cu20Co2	351	16.44	0.333	0.0640	0.170	0.0735
La60Al20Co20	477	15.96	0.335	0.0585	0.158	0.0674
Pr55Al25Co20	509	15.07	0.341	0.0548	0.155	0.0639
Dy55Al25Co20	635	14.27	0.304	0.0636	0.141	0.0706
Tb55Al25Co20	612	14.15	0.302	0.0635	0.140	0.0704
Ho55Al25Co20	649	13.85	0.311	0.0652	0.151	0.0730
Er55Al25Co20	663	13.55	0.306	0.0665	0.149	0.0740
Tm39Y16Al25Co20	664	13.51	0.305	0.0726	0.162	0.0807
Tm55Al25Co20	678	13.47	0.319	0.0612	0.148	0.0690
Lu39Y16Al25Co20	687	13.30	0.316	0.0699	0.166	0.0785
Lu45Y10Al25Co20	698	13.25	0.307	0.0710	0.160	0.0790
Lu55Al25Co20	701	13.20	0.307	0.0693	0.157	0.0772
Mg65Cu25Gd10	421	12.51	0.313	0.0689	0.161	0.0772
Mg65Cu25Y9Gd1	423	12.37	0.277	0.0718	0.137	0.0777
Mg65Cu25Y10	419	12.36	0.302	0.0669	0.147	0.0741
Mg65Cu25Y8Gd2	420	12.23	0.284	0.0705	0.140	0.0767
Mg65Cu25Y5Gd5	422	12.05	0.284	0.0677	0.134	0.0737
Mg65Cu25Tb10	415	11.95	0.309	0.0680	0.155	0.0758
Zr64.13Cu15.75Ni10.12Al10	640	11.68	0.377	0.0624	0.234	0.0779
Zr65Cu15Ni10Al10	652	11.65	0.37	0.0651	0.229	0.0799
Zr61.88Cu18Ni10.12Al10	651	11.51	0.377	0.0618	0.230	0.0770
Zr55Al19Co19Cu7	733	11.44	0.377	0.0579	0.216	0.0720
Zr57Nb5Cu15.4Ni12.6Al10	687	11.44	0.365	0.0641	0.216	0.0777
Zr57Ti5Cu20Ni8Al10	657	11.43	0.362	0.0629	0.207	0.0760
(Zr59Ti6Cu22Ni13)85.7Al14.3	689	10.74	0.363	0.0637	0.211	0.0770
Cu45Zr45Al7Gd3	670	10.71	0.358	0.0637	0.204	0.0764
Zr46.75Ti8.25Cu10.15Ni10Be27.25	622	10.21	0.35	0.0734	0.221	0.0867
Zr48Nb8Cu12Fe8Be24	658	10.17	0.36	0.0654	0.211	0.0785
Zr41Ti14Cu12.5Ni10Be22.5	625	9.79	0.352	0.0705	0.215	0.0835
Ni45Ti20Zr25Al10	733	9.61	0.359	0.0634	0.204	0.0760
Cu60Zr20Hf10Ti10	754	9.50	0.369	0.0559	0.194	0.0684
Pd77.5Cu6Si16.5	633	8.74	0.41	0.0528	0.276	0.0729
Pd64Ni16P20	630	8.29	0.408	0.0517	0.263	0.0707
Pd40Cu40P20	590	7.98	0.402	0.0540	0.257	0.0723
Pd39Ni10Cu30P21	560	7.97	0.397	0.0601	0.272	0.0791
Fe53Cr15Mo14Er1C15B6	900	7.94	0.317	0.0734	0.191	0.0840
Fe61Mn10Cr4Mo6Er1C15B6	930	7.48	0.281	0.0725	0.141	0.0787

the elastic model, the $\Delta E(T_g)/k_B T_g$ is a constant for different MGs, and the ΔE is related to elastic moduli M: $\Delta E(T_g) \propto M(T_g)$. Therefore, $M(T_g)/T_g$ should be a constant for MGs. That is, for various MGs, T_g is closely related to the G or E as experimental results have shown.[16,43,45] From the construction of the fragility plot, all viscosity curves intersect at T_g [Ref. 108]. This means that if a liquid has a steeper slope of $log\eta$ near T_g, it inevitably has a smaller slope of $log\eta$ at high temperature. At high temperatures, relaxation in most of the liquids shows Arrhenius temperature dependence: $\eta = \eta_0 \exp(\Delta E/T)$. Thus, the high-$T$ slope of $\log\eta$ in the fragility plot, $\Delta E/T_g$, can also be a measure of fragility. Experimental data show that $\Delta E/T_g$ indeed roughly correlates with fragility m in various glasses:[105] $T_g/\Delta E \propto m$. Therefore, according to elastic model, both ΔE and T_g correlate with elastic moduli as experimental observed.[14,16]

The correlation between fragility and glass-forming ability has been found in many MG-forming systems[109–112] can be understood from the elastic model. On the other hand, the fragility correlates with the Poisson's ratio in MGs.[16] The Poisson's ratio then can be regarded as an indicator of the glass-forming ability of an alloy. Because the average

Author complimentary copy. Redistribution subject to AIP license or copyright, see http://jap.aip.org/jap/copyright.jsp

barrier for flow ΔE is mainly related to G,[81,82] for the MG-forming systems with low G or larger Poisson's ratio, their ΔE is easy to be surmounted via small strain energy. While surmounting the large energy barrier (small v) will take some finite time and large energy, in order for the system to track the changes in the PEL through structural rearrangements. For example, in Fe-based MGs with low Poisson's ratio, there is tendency to suggest that glass-forming ability is enhanced by increasing of energy barrier.[113] Therefore, an alloy development strategy relies on dramatically increasing flow activation energy, or increasing GV_m or decreasing v, which result in high glass-forming ability in an alloy. The elastic model also offers a simple scenario for explaining the found correlation between T_g and Debye temperature θ_D^2 in MGs.[16,94] One of the long-standing controversial issues is the formation mechanism of shear bands involving viscosity drop during shear banding.[113] The softening has been attributed to mechanical dilatation or shearing.[11,12] Due to the formation of shear bands that is akin to the process of glass transition, according to the elastic model, both the shear flow and the dilatation should be involved in the formation of shear bands. The elastic model also has implication for the design of plastic metallic glasses. To decrease the activation barrier or G, one can enhance the plasticity of a MG. This is in agreement with the fact that a higher Poisson's ratio represents a higher possibility for a MG to have better toughness.[14]

IV. SUMMARY AND CONCLUSIONS

We show compelling experimental evidence that the activation of the unit of flow event and slow β-relaxations in metallic glasses are directly correlated. The slow β-relaxations can be regarded as a thermal driven process of flow events, and the mechanical yield where the atomic sites are topologically unstable by applied stress can be treated as the stress driven glass transition, and the formation of shear bands is a consequence of the stress-induced glass to supercooled liquid transition. Based on the experimental observations, an elastic perspective of the metallic glasses is suggested as that: the glass formation from solidification of liquid, the mechanical deformation, and relaxation of MGs can be treated as the change of their different configurations or flow, and the flow can be modeled activated hopping between inherent states in the PEL. The energy barriers of the flow of both homogeneous flow and in MG-forming liquids and inhomogeneous flow in MG, or the variation in the configurational change or flow of liquid induced either by thermal excitation or mechanical stress, are determined with instantaneous elastic moduli.

An extended elastic model is then proposed to describe the flow both in MGs and MG-forming liquids based on the PEL theory. The activation energy density ρ_E is determined to be a simple expression of $\rho_E = \frac{10}{11}G + \frac{1}{11}K$. That is, both shear and bulk moduli are critical parameters accounting for both homogeneous and inhomogeneous flows in MGs and MG-forming liquids. The extended elastic model has been verified by experiments. It is therefore concluded that the elastic moduli are the key physical parameters for controlling the main thermodynamic and kinetic, mechanical and physical properties of metallic supercooled liquids and MGs, and for understanding and characterizing the MGs. The elastic model might offer a realistic and simple picture for understanding the glass transition and deformation, and the natures in MGs and MG-forming liquids.

ACKNOWLEDGMENTS

We thank the experimental assistance and discussions from H. B. Yu, J. Q. Wang, H. B. Ke, P. Wen, R. J. Wang, and H. Y. Bai, and discussions with T. G. Nieh, M. W. Chen, and Y. Wu. The critical comments of the anonymous reviewer are appreciated. Financial support is from the NSF of China (Nos. 50731008 and 50921091) and MOST 973 of China (Nos. 2007CB613904 and 2010CB731603).

[1] C. A. Angell, Science **267**, 1924 (1995).
[2] G. Tammann, J. Soc. Glass Tech. **9**, 166 (1925).
[3] M. Goldstein, J. Chem. Phys. **51**, 3728 (1969).
[4] P. G. Debenedetti and F. H. Stillinger, Nature **410**, 259 (2001).
[5] M. H. Cohen and D. Turnbull, J. Chem. Phys. **31**, 1164 (1959).
[6] G. Adam and J. H. Gibbs, J. Chem. Phys. **43**, 139 (1965).
[7] J. C. Dyre, Rev. Mod. Phys. **78**, 953 (2006).
[8] S. V. Nemilov, Russ. J. Phys. Chem. **42**, 2673 (1968).
[9] A. L. Greer and E. Ma, MRS Bull. **32**, 611 (2007).
[10] C. A. Schuh, T. C. Hufnagel, and U. Ramamurty, Acta Mater. **55**, 4067 (2007).
[11] A. S. Argon, Acta Metall. **27**, 47 (1979).
[12] F. Spaepen, Acta Metall. **25**, 407 (1977).
[13] W. L. Johnson and K. Samwer, Phys. Rev. Lett. **95**, 195501 (2005).
[14] J. J. Lewandowski, W. H. Wang, and A. L. Greer, Philos. Mag. Lett. **85**, 77 (2005).
[15] M. L. Falk and J. S. Langer, Phys. Rev. E **57**, 7192 (1998).
[16] W. H. Wang, J Appl. Phys. **99**, 093506 (2006).
[17] D. Pan, A. Inoue, T. Sakurai, and M. W. Chen, Proc. Natl. Acad. Sci. USA **105**, 4769 (2008).
[18] J. C. Dyre and N. B. Olsen, Phys. Rev. E **69**, 042501 (2004).
[19] W. H. Wang, Prog. Mater. Sci. **52**, 540 (2007).
[20] W. H. Wang, Adv. Mater. **21**, 4524 (2009).
[21] Q. Luo and W. H. Wang, J. Non-Cryst. Solids **355**, 759 (2009).
[22] G. P. Johari and M. Goldstein, J. Chem. Phys. **53**, 2372 (1970).
[23] L. N. Hu and Y. Z. Yue, J. Phys. Chem. C **113**,15001 (2009).
[24] Z. F. Zhao, P. Wen, C. H. Shek, and W. H. Wang, Phys. Rev. B **75**, 174201 (2007).
[25] R. E. Robertson, J. Chem. Phys. **44**, 3950 (1966).
[26] H. Eyring, J. Chem. Phys. **4**, 283 (1936).
[27] C. D. Xiao, J. Y. Jho, and J. A. F. Yee, Macromolec. **27**, 2761 (1994).
[28] H. B. Yu, W. H. Wang, H. Y. Bai, Y. Wu, and M. W. Chen, Phys. Rev. B **81**, 220201 (2010).
[29] G. E. Dieter, *Mechanical Metallurgy* (McGraw-Hill, New York, 1988).
[30] H. M. Chen, S. X. Song, J. C. Huang, H. S. Chou, J. S. C. Jang, and T. G. Nieh, Appl. Phys Lett. **94**, 141914 (2009).
[31] K. W. Park, C. M. Lee, H. J. Kim, and J. C. Lee, Mater. Sci. Eng. A **499**, 529 (2009).
[32] J. G. Wang, D. Q. Zhao, M. X. Pan, W. H. Wang, S. X. Song, and T. G. Nieh, Scripta Mater. **62**, 477 (2010).
[33] H. B. Ke, P. Wen, D. Q. Zhao, and W. H. Wang. Appl. Phys. Lett. **96**, 251902 (2010).
[34] S. Li, R. J. Wang, M. X. Pan, D. Q. Zhao, and W. H. Wang, J. Non-Cryst. Solids **354**, 1080 (2008).
[35] K. W. Park, C. M. Lee, M. Wakeda, Y. Shibutani, M. L. Falk, and J. C. Lee, Acta Mater. **56**, 5440 (2008).
[36] P. D. Hey, J. Sietsma, and A. V. D. Beukel, Acta Mater. **46**, 5873 (1998).
[37] N. Hirai and H. Eyring, J. Polymer Sci. **37**, 51 (1959).
[38] R. Busch, W. Liu, and W. L. Johnson, J Appl. Phys. **83**, 4134 (1998).
[39] R. Busch, Y. J. Kim, W. L. Johnson, A. J. Rulison, W. K. Rhim, and D. Isheim, Appl. Phys. Lett. **66**, 3111 (1995).
[40] W. N. Myung, H. Y. Bae, I. S. Hwang, H. G. Kim, N. Nishiyama, A. Inoue, and A. L. Green, Mater. Sci. Eng. A **304**, 687 (2001).

Author complimentary copy. Redistribution subject to AIP license or copyright, see http://jap.aip.org/jap/copyright.jsp

[41]H. S. Chen, H. Kato, A. Inoue, J. Saida, and N. Nishiyama, Appl. Phys. Lett. **79**, 60 (2001).
[42]G. J. Fan, M. Freels, H. Choo, P. K. Liaw, P. K. J. J. Z. Li, W. Rhim, W. L. Johnson, and W. H. Wang, Appl. Phys. Lett. **89**, 241917 (2006).
[43]Y. H. Liu, C. T. Liu, W. H. Wang, A. Inoue, T. Sakurai, and M. W. Chen, Phys. Rev. Lett. **103**, 065504 (2009).
[44]B. Yang, C. T. Liu, and T. G. Nieh, Appl. Phys. Lett. **88**, 221911 (2006).
[45]W. H. Wang, J. Non-Cryst. Solids **351**, 1481 (2005).
[46]J. Q. Wang, W. H. Wang, H. B. Yu, and H. Y. Bai, Appl. Phys. Lett. **94**, 121904 (2009).
[47]S. G. Mayr, Phys. Rev. Lett. **97**, 195501 (2006).
[48]H. N. Lee, K. Paeng, S. F. Swallen, and M. D. Ediger, Science **323**, 231 (2009).
[49]J. S. Harmon, M. D. Demetriou, W. L. Johnson, and K. Samwer, Phys. Rev. Lett. **99**, 135502 (2007).
[50]A. J. Liu and S. R. Nagel, Nature **396**, 21 (1998).
[51]D. A. Weitz, Science **323**, 214 (2009).
[52]P. F. Guan, M. W. Chen, and T. Egami, Phys. Rev. Lett. **104**, 205701 (2010).
[53]O. N. Senkov, Phys. Rev. B **76**, 104202 (2007).
[54]K. L. Ngai and S. Capaccioli, Phys. Rev. E **69**, 031501 (2004).
[55]Y. Li, P. Yu, and H. Y. Bai, J. Appl. Phys. **104**, 013520 (2008).
[56]J. Lu, G. Ravichandran, and W. L. Johnson, Acta Mater. **51**, 3429 (2003).
[57]M. Bletry, P. Guyot, J. J. Blandin, and J. L. Soubeyroux, Acta Mater. **54**, 1257 (2006).
[58]M. Heggen, F. Spaepen, and M. Feuerbacher, J. Appl. Phys. **97**, 033506 (2004).
[59]B. Gun, K. J. Laws, and M. Ferry, J. Non-Cryst. Solids **352**, 3896 (2006).
[60]K. S. Lee, H. J. Jun, S. Pauly, B. Bartusch, Y. W. Chang, and J. Eckert, Intermetall**.** **17**, 65 (2009).
[61]Y. Kawamura, T. Nakamura, and A. Inoue, Scripta Mater. **39**, 301 (1998).
[62]Y. Kawamura, T. Nakamura, and A. Inoue, Mater. Trans. JIM. **40**, 794 (1999).
[63]J. D. Eshelby, Proc. Roy. Soc. London **241**, 376 (1957).
[64]K. Zhao, X. X. Xia, H. Y. Bai, D. Q. Zhao, and W. H. Wang, Appl. Phys. Lett. **98**, 141913 (2011).
[65]P. Wen, D. Q. Zhao, M. X. Pan, and W. H. Wang, Appl. Phys. Lett. **84**, 2790 (2004).
[66]J. M. Pelletier, B. Van de Moortele, and I. R. Lu, Mater. Sci. Eng. A **336**, 190 (2002).
[67]J. Schroers, B. Lohwongwatana, A. Peker, and W. L. Johnson, Appl. Phys. Lett. **87**, 061912 (2005).
[68]J. F. Li, D. Q. Zhao, and W. H. Wang, Appl. Phys. Lett. **93**, 171907 (2008).
[69]B. Zhang, D. Q. Zhao, M. X. Pan, W. H. Wang, and A. L. Greer, Phys. Rev. Lett. **94**, 205502 (2005).
[70]Y. T. Wang, H. Y. Bai, and W. H. Wang, Sci. China G **51**, 337 (2008).
[71]X. J. Gu, A. G. McDermott, S. J. Poon, and G. J. Shiflet, Appl. Phys. Lett. **88**, 211905 (2006).
[72]M. D. Demetriou, D. C. Hofmann, H. Kozachkov, A. Wiest, J. P. Schramm, and W. L. Johnson, Appl. Phys. Lett. **95**, 041907 (2009).
[73]U. Harms, O. Jin, and R. B. Schwarz, J. Non-Cryst. Solids **317**, 200 (2003).
[74]Y. H. Liu, G. Wang, R. J. Wang, D. Q. Zhao, M. X. Pan, and W. H. Wang, Science **315**, 1385 (2007).
[75]T. Ichitsubo, E. Matsubara, T. Yamamoto, H. S. Chen, N. Nishiyama, J. Saida, and K. Anazawa, Phys. Rev. Lett. **95**, 245501 (2005).
[76]J. G. Wang, D. Q. Zhao, M. X. Pan, C. H. Shek, and W. H. Wang, Appl. Phys. Lett. **94**, 031904 (2009).
[77]M. Reiner. Phys. Today. **17**(1), 62 (1964).
[78]D. J. Wales, *Energy Landscapes* (Cambridge University Press, Cambridge, 2003).
[79]F. H. Stillinger. Science **267**, 1935 (1995).
[80]J. Frenkel, Z. Phys. **37**, 572 (1926).
[81]J. Q. Wang, W. H. Wang, and H. Y. Bai, J. Non-Cryst. Solids **357**, 223 (2011).
[82]J. Q. Wang, W. H. Wang, Y. H. Liu, and H. Y. Bai, Phys Rev. B **83**, 012201 (2011).
[83]E.S.R. Gopal, *Specific Heats at Low Temperatures* (Plenum, New York, 1966).
[84]M. L. Falk, Phys. Rev. B **60**, 7062 (1999).
[85]F. Spaepen, Nature Mater. **5**, 7 (2006).
[86]B. Zhang, H. Y. Bai, Y. Wu, and W. H. Wang, Phys. Rev. B **76**, 012201 (2007).
[87]H. B. Ke, P. Wen, W. H. Wang, and A. L. Greer, Scripta Mater. **64**, 966 (2011).
[88]L. Sun, M. Q. Jiang, and L. H. Dai, Scripta Mater. **63**, 945 (2010).
[89]T. Egami, S. J. Poon, Z. Zhang, and V. Keppens, Phys. Rev. B **76**, 024203 (2007).
[90]L. Battezzati, A. Castellero, and P. Rizzi, J. Non-Cryst. Solids **353**, 3318 (2007).
[91]H. S. Chen, Appl. Phys. Lett. **29**, 328 (1976).
[92]A. Concustell, F. O. Méar, S. Suriñach, M. D. Baró, and A. L. Greer, Philos. Mag. Lett. **89**, 831 (2009).
[93]S. S. Tsao and F. Spaepen, Acta Metall. **33**, 881 (1985).
[94]W. H. Wang, Z. X. Bao, and J. Eckert, Phys. Rev. B **61**, 3166 (2000).
[95]L. M. Wang, W. H. Wang, R. J. Wang, Z. J. Zhan, D. Y. Dai, L. L. Sun, and W. K. Wang, Appl. Phys. Lett. **77**, 1147 (2000).
[96]D. W. Taylor, *Fundamentals of Soil Mechanics* (Wiley, New York, 1948).
[97]D. Deng and B. Lu, Scripta Metall. **17**, 515 (1983).
[98]A. S. Argon, J. Megusar, and N. J. Grant, Scripta Metall. **19**, 591 (1985).
[99]W. H. Wang, R. J. Wang, F. Y. Li, D. Q. Zhao, and M. X. Pan, Appl. Phys. Lett. **74**, 1803 (1999).
[100]B. Zhang, D. Q. Zhao, M. X. Pan, R, J. Wang, and W. H. Wang. Acta Mater. **54**, 3025 (2006).
[101]W. H. Wang, P. Wen, and R. J. Wang, J. Mater. Res. **18**, 2747 (2003).
[102]X. F. Liu and W. H. Wang, Scripta Mater. **62**, 254 (2010).
[103]T. Ichitsubo, W. Itaka, E. Matsubara, H. Kato, S. Biwa, S. Hosokawa, K. Matsuda, J. Saida, and A.Q.R. Baron, Phys. Rev. B **81**, 172201 (2010).
[104]J. D. Plummer and I. Todd, Appl. Phys. Lett. **98**, 021907 (2011).
[105]V. N. Novikov and A. P. Sokolov. Phys. Rev. B **74**, 064203 (2006).
[106]S. J. Poon, A. Zhu, and G. J. Shiflet, Appl. Phys. Lett. **92**, 261902 (2008).
[107]Z. Lu and J. Li, Appl. Phys. Lett. **94**, 061913 (2009).
[108]M. R. Barrer, Trans. Faraday Soc. **39**, 48 (1943).
[109]O. N. Senkov, Phys. Rev. B **76**, 104202 (2007).
[110]Q. G. Meng, S. G. Zhang, M. X. Xia, J. G. Li, and J. K. Zhou, Appl. Phys. Lett. **90**, 031910 (2007).
[111]M. D. Memetriou, G. Kaltenboeck, J. Y. Suh, G. Garrett, M. Floyd, C. Crewdson, D. C. Hofmann, H. Kozachkov, A. Wiest, J. P. Schramm, and W. L. Johnson, Appl. Phys. Lett. **95**, 041907 (2009).
[112]Y. Wang, H. R. Geng, and Z. X. Yang, J. Non-Cryst. Solids **354**, 3984 (2008).
[113]F. Spaepen, Nature Mater. **5**, 7 (2006).

Author complimentary copy. Redistribution subject to AIP license or copyright, see http://jap.aip.org/jap/copyright.jsp